

# Influence of Asymmetric Recurrent Laryngeal Nerve Stimulation on Vibration, Acoustics, and Aerodynamics

Dinesh K. Chhetri, MD; Juergen Neubauer, PhD; Elazar Sofer, MD

**Objectives/Hypothesis:** Evaluate the influence of asymmetric recurrent laryngeal nerve (RLN) stimulation on the vibratory phase, acoustics and aerodynamics of phonation.

**Study Design:** Basic science study using an in vivo canine model.

**Methods:** The RLNs were symmetrically and asymmetrically stimulated over eight graded levels to test a range of vocal fold activation conditions from subtle paresis to paralysis. Vibratory phase, fundamental frequency ( $F_0$ ), subglottal pressure, and airflow were noted at phonation onset. The evaluations were repeated for three levels of symmetric superior laryngeal nerve (SLN) stimulation.

**Results:** Asymmetric laryngeal adductor activation from asymmetric left-right RLN stimulation led to a consistent pattern of vibratory phase asymmetry, with the more activated vocal fold leading in the opening phase of the glottal cycle and in mucosal wave amplitude. Vibratory amplitude asymmetry was also observed, with more lateral excursion of the glottis of the less activated side. Onset fundamental frequency was higher with asymmetric activation because the two RLNs were synergistic in decreasing  $F_0$ , glottal width, and strain. Phonation onset pressure increased and airflow decreased with symmetric RLN activation.

**Conclusion:** Asymmetric laryngeal activation from RLN paresis and paralysis has consistent effects on vocal fold vibration, acoustics, and aerodynamics. This information may be useful in diagnosis and management of vocal fold paresis.

**Key Words:** Recurrent laryngeal nerve, laryngeal asymmetry, high speed video, acoustics, vibration, phonation.

**Level of Evidence:** N/A.

*Laryngoscope*, 124:2544–2550, 2014

## INTRODUCTION

Vocal fold paresis is increasingly recognized as a commonly encountered clinical condition causing dysphonia.<sup>1,2</sup> There is common consensus that laryngeal paresis may go unrecognized during clinical voice evaluation due to the lack of an obvious sign indicative of paresis such as reduced vocal fold mobility.<sup>2,3</sup> Laryngoscopic abnormalities in paresis are subtle, thus necessitating systematic research on the influence of paresis on laryngeal physiology. Previously reported laryngeal findings of paresis in the presence of normally mobile vocal folds have included asymmetry in the alignment of laryngeal cartilages, vocal fold bowing, glottal gap, vocal process height mismatch, false vocal fold hyperadduction, deviation of the epiglottic petiole, and vibratory amplitude abnormalities.<sup>4–7</sup> However, these signs may

not be always present. In addition, laryngeal paresis can be due to recurrent laryngeal nerve (RLN) deficit, superior laryngeal nerve (SLN) deficit, or both, thus making it challenging to detect and/or determine the side of paresis.

Laryngeal videostroboscopy remains the most commonly used endoscopic procedure for clinical evaluation of dysphonia.<sup>8</sup> The power of videostroboscopy is its ability to allow real-time clear visualization of (a) the medial vocal fold vibratory edge and (b) the mucosal wave, an apparent travelling “wave” of mucosal upheaval on the vocal fold surface during phonation that is visualized due to the vertical phase delay of the upper and lower margins of glottal closure.<sup>9</sup> Although the presence of the mucosal wave is indicative of the pliability of the vocal fold cover layer, the characteristics of the travelling wave also carries useful information regarding the overall tension or stiffness of the vocal fold. Vocal fold paresis and paralysis lead to reduced vocal fold stiffness, which is expected to have direct consequences on vibratory properties.<sup>10,11</sup> Three vibratory characteristics relevant to vocal fold paresis and paralysis can be assessed: the *phase* of vibration, assessed as the symmetry (or lack thereof) of the excursion of the vocal fold medial edge during the opening and closing phases of the glottal cycle; *mucosal wave amplitude*, noted as the most lateral excursion of the visible mucosal wave on the superior vocal fold surface; and the *vibratory amplitude*, noted as the most lateral displacement of the vocal fold medial edge during the glottal cycle.<sup>8,9</sup>

From the Laryngeal Physiology Laboratory, Department of Head and Neck Surgery, UCLA School of Medicine, Los Angeles, California, U.S.A.

Editor's Note: This Manuscript was accepted for publication May 20, 2014.

Presented as an oral presentation at The Triological Society Combined Sections Meeting, Miami, Florida, January 10–12, 2014.

This study was supported by a grant from the National Institutes of Health (no. RO1 DC011300). The authors have no other funding, financial relationships, or conflicts of interest to disclose.

Send correspondence to Dinesh K. Chhetri, MD, Laryngeal Physiology Laboratory, CHS 62-132, Department of Head and Neck Surgery, UCLA School of Medicine, 10833 Le Conte Avenue, Los Angeles, CA 90095. E-mail: dchhetri@mednet.ucla.edu

DOI: 10.1002/lary.24774

Systematic studies of the influence of vocal fold adductor paresis as an independent variable on laryngeal function have not been performed. Thus, laryngeal vibratory characteristics have not been commonly used in making the diagnosis of paresis. Previously, we demonstrated that vocal fold tension asymmetry due to asymmetric cricothyroid (CT) muscle activation by asymmetric SLN stimulation leads to a consistent pattern of vibratory phase asymmetry, with the more activated side leading in phase during glottal opening.<sup>12</sup> In this investigation, we tested the hypothesis that asymmetric activation of laryngeal adductor muscles by asymmetric RLN stimulation also leads to vibratory phase asymmetry. Using an *in vivo* canine model, we tested multiple symmetric and asymmetric vocal-fold adduction activation conditions, and concurrently measured vibration, acoustics, and aerodynamics. The results further the general understanding of phonatory consequences from asymmetric laryngeal activation and are also expected to be clinically useful in the diagnosis of paresis.

## MATERIALS AND METHODS

### *In Vivo Canine Model*

The canine larynx is a close match to the human larynx in its gross, microscopic, and histologic anatomy, and the validity of an *in vivo* canine model is well established in voice research.<sup>9,13,14</sup> This study protocol was approved by the University of California–Los Angeles, Animal Research Committee. Two mongrel canines were used. Surgical exposure of the larynx and the laryngeal nerves was as described in detail previously.<sup>12,13</sup> In brief, the larynx was exteriorized in the neck; the laryngeal nerves were dissected; and a tracheostomy placed for intraoperative ventilation. The nerve branches to the posterior cricoarytenoid muscles, Galen's anastomosis, and the internal SLN branches were divided bilaterally to eliminate their effects during nerve stimulation. Tripolar cuff electrodes (Ardiem Medical, Indiana, PA) were placed around the RLNs and the external branches of the SLNs.

Graded stimulation was applied to the laryngeal nerves, as described previously, from threshold muscle activation (just a hint of vocal fold movement or strain change) to maximal activation (point of saturation of vocal fold displacement or strain change).<sup>12,13</sup> Each RLN was stimulated over seven levels of graded stimulation (total 8 levels including zero stimulation condition) in a semi-random pattern to obtain 64 distinct left-right RLN activation conditions. The same activation conditions were evaluated for three levels of bilaterally symmetric SLN stimulation (levels 1–3). Neuromuscular stimulation duration for each condition was 1,500 ms with 0.1-ms unipolar cathodic pulses at pulse repetition rate of 100 Hz. To allow muscle recovery and transfer of high speed video data to the host computer, each stimulation pulse train was followed by a 3.5-second pause prior to the next stimulation.

A subglottal tube to provide rostral airflow for phonation was attached around tracheal ring 4 and connected to an airflow controller (MCS Series Mass Flow Controller; Alicat Scientific, Tucson, AZ). The airflow rate was increased linearly from 300 to 1,400 ml/s from onset to end of nerve stimulation (1,500 ms) such that subglottic pressure ( $P_{\text{sub}}$ ) continuously increased beyond phonation onset pressure ( $P_{\text{th}}$ ) or until maximum airflow was reached. The airflow at the glottic level was 37.5°C and 100% humidified using a heated humidifier (HumiCare 200; Gruendler Medical, Freudenberg, Germany).

### *Measurement of Experimental Parameters*

A high-speed digital video (HSV) camera (Phantom v210; Vision Research Inc., Wayne, NJ) imaged laryngeal deformation and vibration at 3,000 frames per second for the duration of nerve stimulation. The distance from the camera to the larynx remained constant for all conditions. For measurement of glottal posture (glottal distance and strain), India ink was used to mark several landmarks on the vocal fold surface. Glottal distance (Dvp) was measured as the distance between the India ink markings at the vocal processes as a percentage of baseline (unstimulated) condition (see Fig. 7).

Acoustic and aerodynamic data were recorded using a probe tube microphone (Model 4128; Bruel & Kjaer North America, Norcross, GA) and a pressure transducer (MKS Baratron 220D, MKS Instruments, Andover, MA) mounted flush with the inner wall of the subglottic inflow tube. The subglottal acoustic pressure signal was used to determine the fundamental frequency ( $F_0$ ) at phonation onset using Sound Forge acoustic analysis software (Sonic Foundry Sound Forge Version 6.0; Sonic Foundry Inc., Madison, WI). The acoustic signal was manually examined, correlated with glottal opening on HSV, and the first four glottal cycles after onset were used to manually calculate the onset  $F_0$ . The corresponding mean subglottal pressure ( $P_{\text{sub}}$ ) at phonation onset then represented the phonation onset pressure ( $P_{\text{th}}$ ).

To evaluate vibratory characteristics, the HSV files were randomized and reviewed independently by two voice scientists (D.K.C. and E.S.) using the Phantom Camera Control Application software (PCC 1.3; Vision Research Inc., Wayne, NJ). Frame-by-frame analysis of the first few vibratory cycles after phonation onset was performed, and the phase of vibration noted as symmetric or asymmetric. If asymmetric, the vocal fold that led in phase during opening was noted (left vs. right). Mucosal wave amplitude and vibratory amplitude were also noted. No attempt was made to quantify the degree of phase asymmetry and the amplitude of vibration, or to measure the speed of the mucosal wave. In clinical practice, these parameters are also similarly assessed qualitatively by frame-by-frame analysis of the glottal opening phase.

### *Data Presentation and Interpretation*

Muscle activation plots (MAPs) are used to illustrate the data. The MAP contains the left RLN activation levels (0–7) on the y-axis and right RLN activation levels (0–7) on the x-axis. This 8 × 8 plot thus concurrently presents all 64 different RLN activation conditions (8 symmetric; 56 asymmetric) using color coding that allows for a visual qualitative interpretation of data. In addition, isocontour lines representing the same data values are provided for ease of data interpretation. This format has been used previously in voice research and facilitates presentation of data trends when a large number of laryngeal activation conditions are concurrently presented.<sup>12,13</sup> Statistical analysis of data is not appropriate in this setting because data trends are emphasized. The findings are robust, consistent with previously reported studies, and reflect fine experimental control of laryngeal activation and their phonatory consequences.

## RESULTS

Two canines were used for this study and the results were nearly identical. Thus, results are presented from one animal to maintain consistency of data values and trends. Data trend was also similar for the three increasing SLN activation levels; therefore, SLN

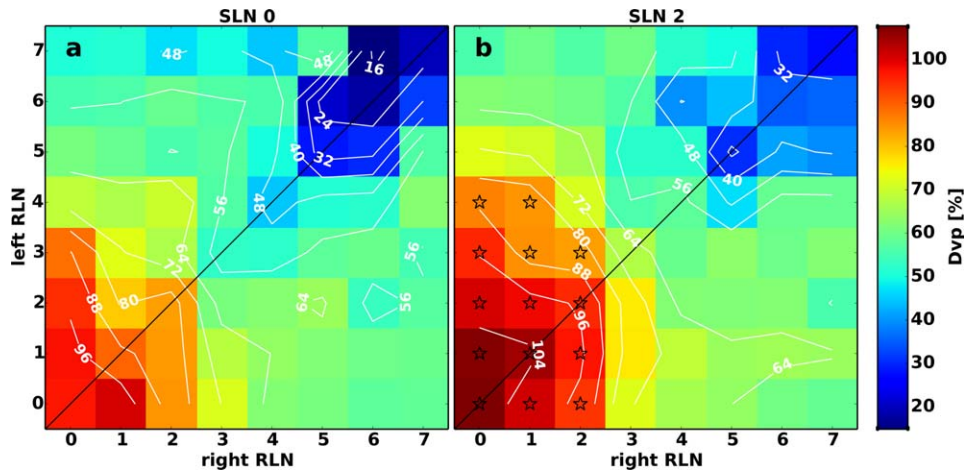


Fig. 1. Muscle activation plot for the relative Dvp from baseline as a function of graded left-right RLN stimulation with (a) zero SLN activation and (b) symmetric midlevel SLN activation. Phonation onset was not reached in the starred areas, but the final glottal distance achieved for these activation conditions is displayed. Dvp = distance between ink marks at vocal processes; RLN = recurrent laryngeal nerves; SLN = superior laryngeal nerves. [Color figure can be viewed in the online issue, which is available at [www.laryngoscope.com](http://www.laryngoscope.com).]

level 2 (mid-level) was chosen to represent the SLN activation conditions.

The relative glottal distance at the vocal processes ( $D_{vp}$ ) compared to baseline condition as a function of left-right RLN stimulation levels is shown in Figure 1. At zero SLN activation (Fig. 1a),  $D_{vp}$  decreased symmetrically with left-right RLN stimulation, illustrating symmetry of the graded levels for glottal closure. With SLN activation, this symmetry was maintained but with slightly more open glottis (Fig. 1b). The influence on onset fundamental frequency ( $F_0$ ) is shown in Figure 2. The isocontour lines reveal that there is a sharp decrease in  $F_0$  while RLN activation is increased, but the magnitude is more pronounced with SLN activation. Higher unilateral RLN activation could also produce the sudden  $F_0$  decrease at zero SLN stimulation, but this was not possible even with maximal unilateral RLN activation with SLN activation (Fig. 2b). At zero SLN activation, all activation conditions including zero RLN levels reached phonation onset. However, when the CT

was activated many low RLN activation conditions did not reach phonation onset at the airflow levels used (starred activation conditions with blank data in Fig. 2b). The decrease in  $F_0$  with RLN activation was primarily associated with decreased strain (data not shown) and is consistent with previous studies.<sup>12,13</sup>

The effects on phonation onset pressure ( $P_{th}$ ) are shown in Figure 3. At zero SLN activation (Fig. 3a), higher  $P_{th}$  values are found in the laryngeal activation levels spanning symmetric RLN stimulation (black diagonal line), whereas decreased onset pressures are found in the asymmetrically activated regions. A slight asymmetry is revealed because right RLN stimulation is able to lower  $P_{th}$  values by a greater magnitude than left RLN activation (Fig. 3a). With SLN activation,  $P_{th}$  range distribution is somewhat contracted, and the isocontour lines reveal no obvious pattern. Increasing RLN activation also led to a consistent decrease in onset airflow (Fig. 4). Symmetric conditions required slightly less airflow compared to asymmetric conditions, and this effect

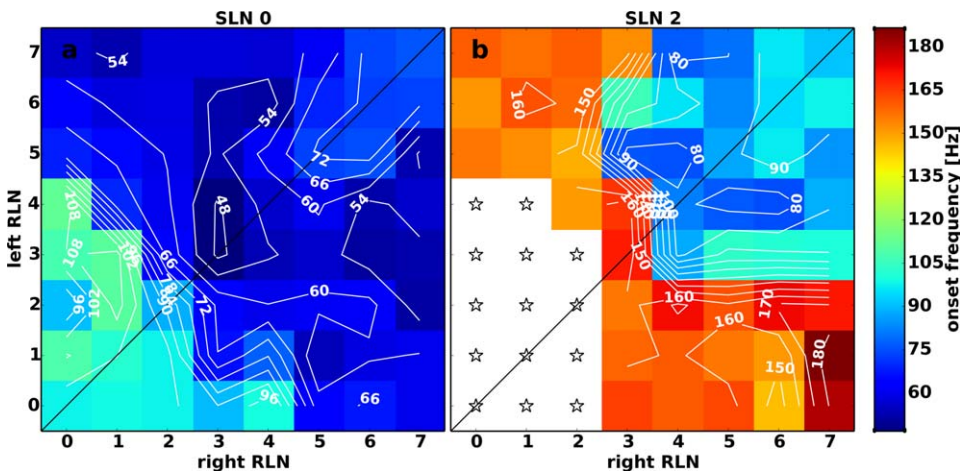


Fig. 2. Muscle activation plot for phonation onset  $F_0$  as a function of graded left-right RLN stimulation with (a) zero SLN activation and (b) symmetric midlevel SLN activation. Phonation onset was not reached in the starred areas.  $F_0$  = fundamental frequency; RLN = recurrent laryngeal nerves; SLN = superior laryngeal nerve. [Color figure can be viewed in the online issue, which is available at [www.laryngoscope.com](http://www.laryngoscope.com).]

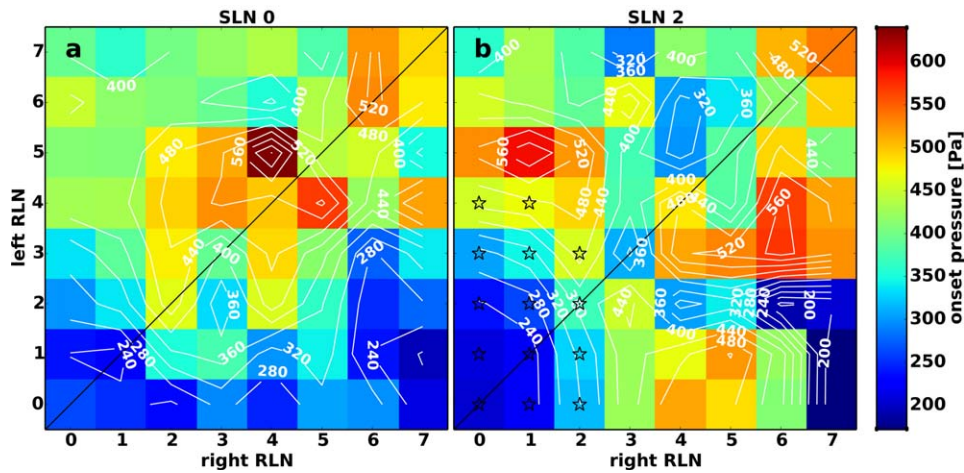


Fig. 3. Muscle activation plot for subglottic pressure at phonation onset ( $P_{th}$ ) as a function of graded left-right RLN stimulation with (a) zero SLN activation and (b) symmetric mid-level SLN activation. Phonation onset was not reached in the starred areas, but the highest subglottal pressure reached in these activation conditions is displayed. P<sub>th</sub> = phonation onset; RLN = recurrent laryngeal nerves; SLN = superior laryngeal nerve. [Color figure can be viewed in the online issue, which is available at [www.laryngoscope.com](http://www.laryngoscope.com).]

was more dramatic with SLN activation (Fig 4b). The highest airflow rates are found adjacent to activation conditions where phonation onset was not reached (starred areas).

The phase of glottal opening revealed a slight right RLN dominance (Fig. 5). At zero SLN stimulation, phase lead was right-sided in all of the seven symmetrically activated conditions (black diagonal line). When the symmetry line was shifted one level to the left toward the actual line of symmetry (white diagonal line), the opening phase was symmetric in six of eight conditions: left leading in one of eight conditions, and right leading in one of eight conditions (Fig. 5a). Otherwise there was a clear preponderance for left phase lead in left more activated conditions, and for right phase lead in right more activated conditions. This pattern of phase lead was maintained upon SLN activation (Fig. 5b). Mucosal

wave amplitude followed phase lead in nearly all instances (Fig. 6). Incidentally the phase lead in the second canine was slightly left-dominant (data not shown).

High-speed video (Fig. 7) and digital kymograms (DKGs) (Fig. 8) clarified the above findings; three illustrative cases are presented. Figures 7A and 8A show the laryngeal activation condition L RLN 6 R RLN 0, where the left fold opened earlier and the mucosal wave travelled farther. Figures 7C and 8C show the laryngeal activation condition L RLN 0 R RLN 6, where the right vocal fold opened earlier and the mucosal wave travelled farther. Figures 7B and 8B show the laryngeal activation condition L RLN 6 R RLN 5 (from the actual line of symmetry), where phase and mucosal wave amplitude are symmetric. The DKGs also further illustrate the amplitude asymmetry, where the medial edge of the less-activated vocal fold travels farther laterally. In

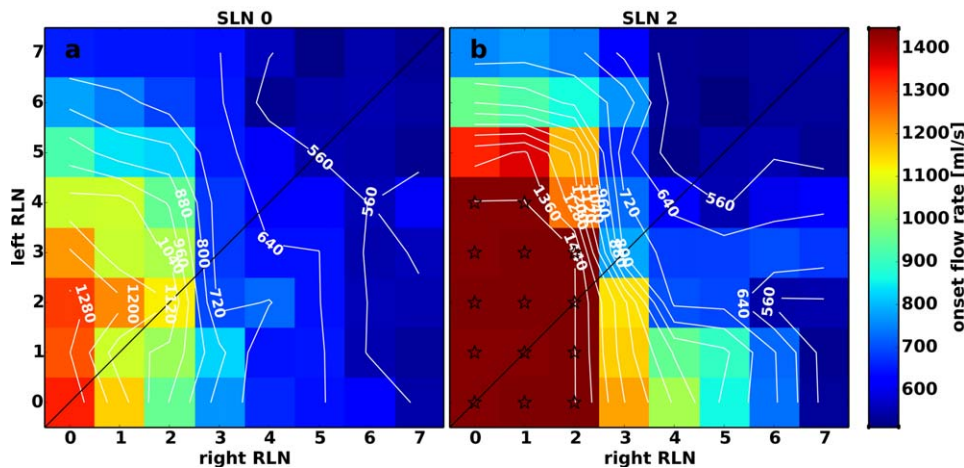


Fig. 4. Muscle activation plot for airflow at phonation onset as a function of graded left-right RLN stimulation with (a) zero SLN activation and (b) symmetric midlevel SLN activation. Phonation onset was not reached in the starred areas, but the highest airflow reached in these activation conditions is displayed. RLN = recurrent laryngeal nerves; SLN = superior laryngeal nerve. [Color figure can be viewed in the online issue, which is available at [www.laryngoscope.com](http://www.laryngoscope.com).]

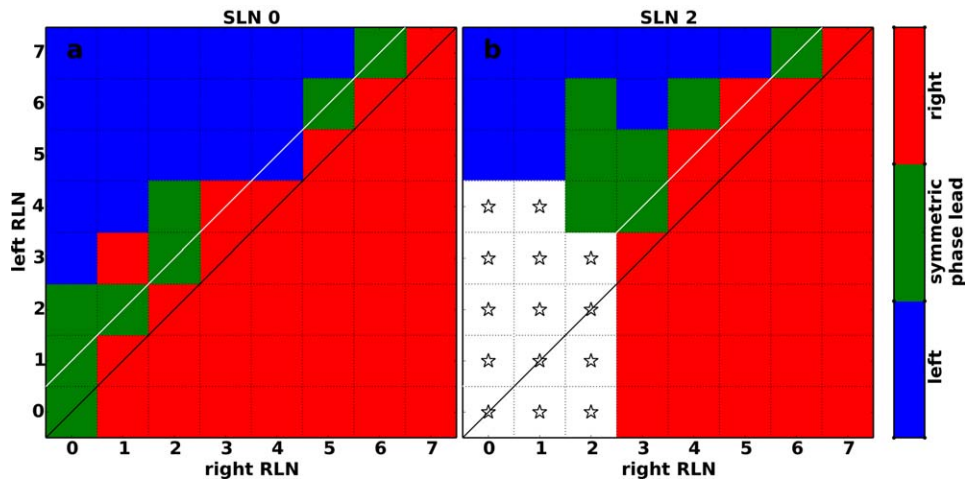


Fig. 5. Muscle activation plot for phase lead at glottal opening as a function of graded left-right RLN stimulation with (a) zero SLN activation and (b) symmetric midlevel SLN activation. The black diagonal line represents the experimental line of symmetry and the white diagonal line represents the actual line of symmetry. Phonation onset was not reached in the starred areas. RLN = recurrent laryngeal nerves; SLN = superior laryngeal nerve. [Color figure can be viewed in the online issue, which is available at [www.laryngoscope.com](http://www.laryngoscope.com).]

general, the degree of asymmetry in phase, mucosal amplitude, and vibratory amplitude were greater, whereas RLN asymmetry increased, but no attempt was made to quantitate these due to technical challenges and also due to the lack of a clinically useful methodology to report them.

## DISCUSSION

In this investigation, the influence of laryngeal adductor asymmetry was tested by graded stimulation of the RLNs to evaluate a variety of paresis and paralysis states. RLN stimulation adducts the vocal fold, decreases the glottal width (Fig. 1), and also shortens the vocal fold at higher levels of stimulation (strain data not shown). RLN stimulation decreases  $F_0$ , increases  $P_{th}$ ,

and decreases airflow at phonation onset (Figs. 2–4). These findings are consistent with breathy dysphonia and increased phonatory effort encountered by patients with vocal fold immobility. SLN activation leads to areas of aphonia, likely due to a combination of increased glottal tension and gap, and is antagonistic to RLN effects. This is consistent with previous reports.<sup>12,13</sup>

The stiffness of the vocal fold body and cover layers are controlled by activation of the intrinsic laryngeal muscles. Specifically, the CT muscles elongate the vocal fold and stiffens the cover layer, whereas the thyroarytenoid muscle stiffens the body layer and shortens the vocal fold at higher activation levels, thus decreasing the tension.<sup>15</sup> Therefore, the activation state of the laryngeal muscles directly affects the mucosal wave properties.<sup>16</sup> This study supports the contention that

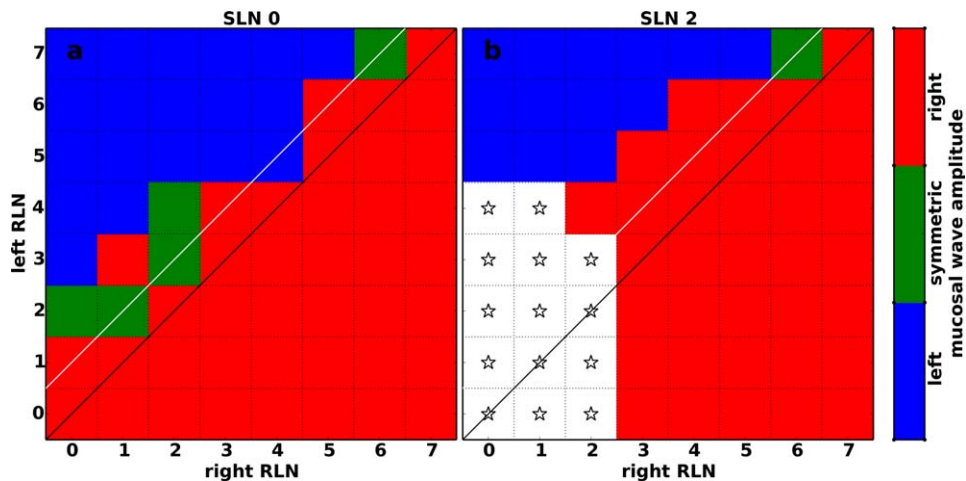


Fig. 6. Muscle activation plot for mucosal wave amplitude as a function of graded left-right RLN stimulation with (a) zero SLN activation and (b) symmetric midlevel SLN activation. The black diagonal line represents the experimental line of symmetry, and the white diagonal line represents the actual line of symmetry. Phonation onset was not reached in the starred areas. RLN = recurrent laryngeal nerves; SLN = superior laryngeal nerve. [Color figure can be viewed in the online issue, which is available at [www.laryngoscope.com](http://www.laryngoscope.com).]

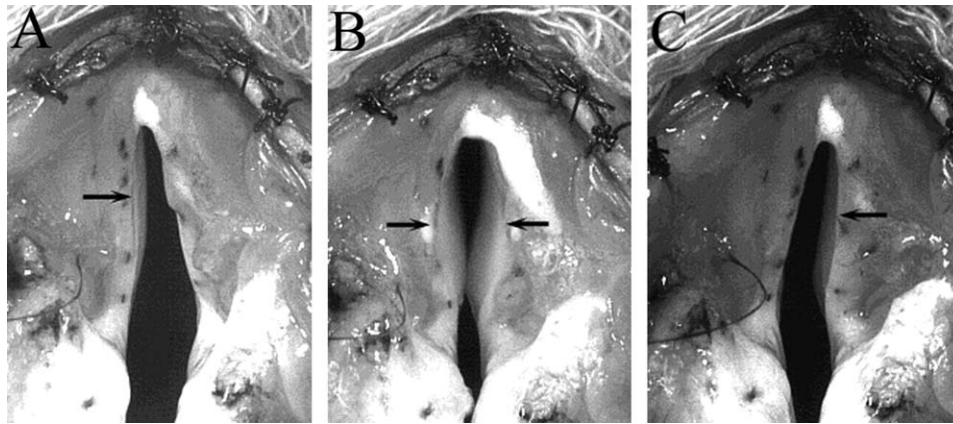


Fig. 7. Glottal opening phase demonstrating mucosal wave excursion on the superior vocal fold surface (arrows). (A) Condition left RLN 6 right 0: The left vocal fold opened earlier and a robust mucosal wave is present on the left. (B) Condition left RLN 6 and right RLN 5: There was symmetric opening phase and mucosal wave amplitude. (C) Condition left RLN 0 and right RLN 6: The right vocal fold opened earlier and a robust mucosal wave is present on the right. These activation conditions correspond to those in Figures 5 and 6. RLN = recurrent laryngeal nerves; SLN = superior laryngeal nerve.

unilateral vocal fold paresis and paralysis due to RLN deficit is associated with ipsilateral phase lag at glottal opening, decreased mucosal wave amplitude, and increased vibratory amplitude. This finding is also consistent with the results of vocal fold physical models and computational models.<sup>16</sup>

The hypothesis that phase asymmetry is present in tension asymmetry from asymmetric RLN activation was verified. However, use of vibratory asymmetry to identify vocal fold paresis is currently not commonly used and may be controversial. Simpson et al.<sup>4</sup> evaluated whether vibratory asymmetry was a reliable predictor of paresis by asking three experienced voice clinicians to review videostroboscopies from 19 patients with mobile vocal folds but laryngeal electromyographic evidence of paresis. The raters reviewed only the fully adducted glottis in phonation and noted if asymmetry of vibration (amplitude or mucosal wave) was present, and if present then predicted the side of paresis. The individual reviewer's ability to designate the side of paresis was about 33%, which is less than random guessing. However, this study

does not detail what methods and criteria the reviewers used to determine paresis or asymmetry, although in the discussion it is stated that "conventional thinking suggests that the denervated side will have an increased amplitude and/or mucosal wave due to the laxity of the paretic vocal fold." The present study would concur with their assumptions regarding the vibratory amplitude but not the mucosal wave amplitude. In addition, only 7 of 19 patients (36%) in that study<sup>4</sup> had unilateral LEMG abnormality. In bilateral laryngeal nerve abnormalities the phase lead would be expected to occur on the more activated side. However, all three reviewers in that study predicted multiple video samples to have bilateral paresis. As left/right asymmetry is an inherently relative assessment, bilateral paresis cannot be predicted from assessment of vibratory asymmetry. Thus the reviewers may have selected other anatomic findings to determine presence of paresis.

This study in combination with our prior study on laryngeal asymmetry from asymmetric CT activation, shows that both RLN and SLN paresis/paralysis can

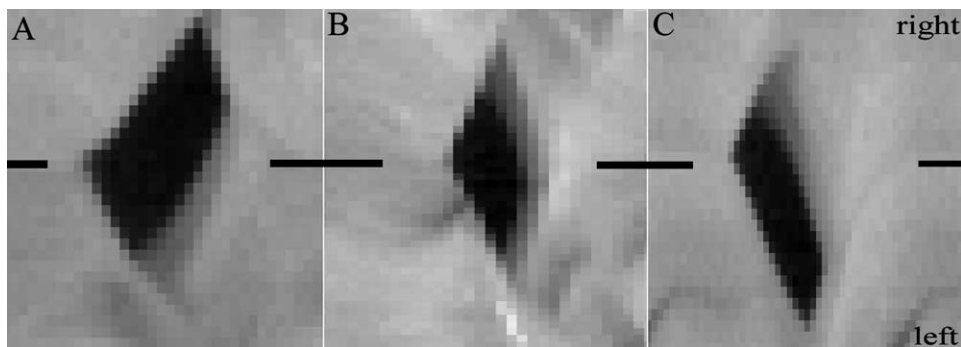


Fig. 8. DKG for the illustrative cases in Figure 7. Glottal midline is designated by the black bars, the top is right vocal fold excursion and the bottom is left vocal fold excursion. (A) Condition left RLN 6 right 0: The left vocal fold led in the opening phase of vibration, but the amplitude of vibration is greater on the right. (B) Condition left RLN 6 right RLN 5: The opening phase and amplitude of vibration are both symmetric. (C) Condition left RLN 0 and right RLN 6: The right vocal fold led in the opening phase of vibration, but the amplitude of vibration is greater on the left. DKG = digital kymograms; RLN = recurrent laryngeal nerves; SLN = superior laryngeal nerve.

lead to similar vibratory abnormalities. The optimal way to look for mucosal wave abnormalities during clinical voice evaluation is to perform frame-by-frame analysis of the opening phase of the glottal cycle. Using this technique the relative side of paresis could be predicted. Although we used high-speed video for this study, videostroboscopy has been shown to be as sensitive for periodic vibration with regard to the vibratory parameters studied in this report.<sup>17</sup> Advancements in real-time videokymography techniques may also allow for this task to be completed with improved accuracy.

## CONCLUSION

Asymmetric left-right RLN stimulation leads to a consistent pattern of vibratory phase asymmetry, with the more activated vocal fold leading in phase during glottal opening. Because vibratory parameters can be assessed by slow motion analysis of the videostroboscopic recording of the glottal opening cycle, this parameter may be useful in clinical evaluation of dysphonia. The side of paresis would be expected to be the side with the phase lag and increased vibratory amplitude. By systematically controlling laryngeal activation and evaluating the influence of paresis in phonation, this study furthers the general understanding of the phonatory consequences of asymmetric laryngeal activation.

## BIBLIOGRAPHY

1. Koufman JA, Postma GN, Cummins MM, Blalock PD. Vocal fold paresis. *Otolaryngol Head Neck Surg* 2000;122:537–541.
2. Sulica L, Blitzer A. Vocal fold paresis: evidence and controversies. *Curr Opin Otolaryngol Head Neck Surg* 2007;15:159–162.
3. Simpson CB, Cheung EJ, Jackson CJ. Vocal fold paresis: clinical and electrophysiologic features in a tertiary laryngology practice. *J Voice* 2009; 23:396–398.
4. Simpson CB, May LS, Green JK, Eller RL, Jackson CE. Vibratory asymmetry in mobile vocal folds: is it predictive of vocal fold paresis? *Ann Otol Rhinol Laryngol* 2011;120:239–242.
5. Sufyan AS, Kincaid JC, Wannemuehler TJ, Halum SL. The interarytenoid spatial relationship: accuracy and interrater reliability for determining sidedness in cases of unilateral adductor paresis. *J Voice* 2013;27:90–94.
6. Tsai V, Celmer A, Berke GS, Chhetri DK. Videostroboscopic findings in unilateral superior laryngeal nerve paralysis and paresis. *Otolaryngol Head Neck Surg* 2007;136:660–662.
7. Roy N, Barton ME, Smith ME, Dromey C, Merrill RM, Sauder C. An in vivo model of external superior laryngeal nerve paralysis: laryngoscopic findings. *Laryngoscope* 2009;119:1017–1032.
8. Mehta DD, Hillman RE. Current role of stroboscopy in laryngeal imaging. *Curr Opin Otolaryngol Head Neck Surg* 2012;20:429–436.
9. Berke GS, Gerratt BR. Laryngeal biomechanics: an overview of mucosal wave mechanics. *J Voice* 1993;7:123–128.
10. Herzel H, Berry D, Titze I, Steinecke I. Nonlinear dynamics of the voice: Signal analysis and biomechanical modeling. *Chaos* 1995;5:30–34.
11. Eysholdt U, Rosanowski F, Hoppe U. Vocal fold vibration irregularities caused by different types of laryngeal asymmetry. *Eur Arch Otorhinolaryngol* 2003;260:412–417.
12. Chhetri DK, Neubauer J, Bergeron JL, Sofer E, Peng KA, Jamal N. Effects of asymmetric superior laryngeal nerve stimulation on glottic posture, acoustics, vibration. *Laryngoscope* 2013;123:3110–3116.
13. Chhetri DK, Neubauer J, Berry DA. Neuromuscular control of fundamental frequency and glottal posture at phonation onset. *J Acoust Soc Am* 2012;131:1401–1412.
14. Garrett CG, Coleman JR, Reinisch L. Comparative histology and vibration of the vocal folds: implications for experimental studies in microlaryngeal surgery. *Laryngoscope* 2000;110:814–824.
15. Hirano M. Morphological structure of the vocal cord as a vibrator and its variations. *Folia Phoniatr (Basel)* 1974;26:89–94.
16. Zhang Z, Luu TH. Asymmetric vibration in a two-layer vocal fold model with left-right stiffness asymmetry: experiment and simulation. *J Acoust Soc Am* 2012;132:1626–1635.
17. Kendall KA. High-speed laryngeal imaging compared with videostroboscopy in healthy subjects. *Arch Otolaryngol Head Neck Surg* 2009;135: 274–281.